Inorg. Chem. **2005**, *44*, 4644–4655

Structural, Magnetic, and Spectroscopic Comparative Studies on Four New Derivatives of DIMMAL (2-Di1*H*-2-imidazolylmethylmalonate): A Novel Generator of Multidimensional Networks

Hugo Núñez, Lucía Soto, Juan Server-Carrió, Julia García-Lozano, Amparo Sancho, Rafael Acerete, and Emilio Escrivà*

Departament de Química Inorgànica, Universitat de València, c/Vicent Andrés Estellés, s/n, 46100 Burjassot (València), Spain

Received December 16, 2004

This paper reports the synthesis, structure solution, and magnetic characterization of four new DIMMAL-containing compounds (H_2DIMMAL = 2-di1*H*-2-imidazolylmethylmalonic acid), H_2DIMMAL·H_2O (**1**), Na_2(DIMMAL)·$5H_2O$ (**2**), [Cu(HDIMMAL)$_2$] (**3**), and [Cu_2(DIMMAL)$_2$(H_2O)$_2$]·$2H_2O$ (**4**). Compound **1**, containing two carboxylates and two protonated imidazole rings, adopts the dizwitterion configuration. These monohydrate MBBs pack together into a 3D array driven, as in the other three cases herein reported, by a combination of multiple-path H-bonds and aromatic–aromatic interactions. Compound **2** consists of centrosymmetric Na^+ tetramers in which four NaO_6 distorted octahedra are interconnected by carboxylate and water bridges. Compound **3** consists of mononuclear [Cu(HDIMMAL)$_2$] units in which HDIMMAL$^-$ acts as a tridentate ligand through two imidazole N atoms and the deprotonated O from a carboxylate. Compound **4** consists of centrosymmetric cyclic dinuclear [Cu_2(DIMMAL)$_2$-(H_2O)$_2$]·$2H_2O$ units involving propionate-arm bridges. The building-block units described above, in each case, are interconnected into 3D networks by multiple H-bonding paths and aromatic–aromatic interactions. The EPR spectra are indicative of an essentially $d_{x^2-y^2}$ ground state for the copper(II) ions in **3** and **4** (CuN_4O_2 and CuN_2O_2O' chromophores, respectively). Magnetic susceptibility measurements in the range of 1.8–200 K for compound **4** show weak antiferromagnetic exchange between the copper(II) ions ($2J = -1.6(1)$ cm^{-1}). The effectiveness of the propionate-arm bridges, involving C–C σ bonds, in propagating magnetic exchange between the copper(II) ions is discussed.

Introduction

The construction of extended 3D networks from small size molecular entities has received increasing attention in recent years. Progress in this field[1] has undoubtedly been fueled by the possibility of designing specific tailor-made molecular building blocks (MBBs) capable of self-associating into a variety of architectures with characteristic network topologies. Two main strategies have been outlined to obtain tailor-made predetermined functional networks through the assembly of MBBs, namely, crystal engineering and reticular synthesis.[1h,n] It is in this context that a considerable effort has been recently made to explore the use of coordination compounds as MBBs that, by an appropriate combination of strong coordinative capacity with weak noncovalent hydrogen bonds and aromatic−aromatic interactions, would provide the directional motifs leading to the self-assembly of new network structures of interest. For this reason, the design and synthesis of new metal−organic frameworks

* To whom correspondence should be addressed. E-mail: escriva@uv.es.

(1) (a) Lehn, J.-M. *Supramolecular Chemistry: Concepts and Perspectives;* VCH: Weinheim, Germany, 1995. (b) Atwood, J. L.; Davies, J. E. D.; MacNicol, D. D.; Vögtle, F.; Lehn, J.-M., Eds. *Comprehensive Supramolecular Chemistry;* Pergamon: Oxford, 1996. (c) Russell, V. A.; Evans, C. C.; Li, W.; Ward, M. D. *Science* **1997**, *276*, 576. (d) Alivisatos, P. L.; Barbara, P. F.; Castleman, A. W.; Chang, J.; Dixon, D. A.; Klein, M. L.; McLendon, G. L.; Miller, J. S.; Ratner, M. A.; Rossky, P. J.; Stupp, S. I.; Thompson, M. E. *Adv. Mater*. **1998**, *10*, 1297. (e) Braga, D. *J. Chem. Soc., Dalton Trans.* **2000**, 3705. (f) Cantrill, S. J.; Pease, A. R.; Stoddart, J. F. *J. Chem. Soc., Dalton Trans.* **2000**, 3715. (g) Lehn, J.-M.; Eliseev, A. *Science* **2001**, *291*, 2331. (h) Moulton, B.; Zaworotko, M. J. *Chem. Rev.* **2001**, *101*, 1629. (i) Desiraju, G. R. *Nature* **2001**, *412*, 399. (j) Desiraju, G. R. *Acc. Chem. Res.* **2002**, *35*, 565. (k) Halder, G. J.; Kepert, C. J.; Moubaraki, B.; Murray, K. S.; Cashion, J. D. *Science* **2002**, *295*, 1762. (l) Lehn, J.-M. *Science* **2002**, *295*, 2400. (m) Reinhoudt, D. N.; Crego-Calama, M. *Science* **2002**, *295*, 2403. (n) Hollingsworth, M. D. *Science* **2002**, *295*, 2410. (o) Yaghi, O. M.; O'Keeffe, M. L.; Ockwig, N. W.; Chae, H. K.; Eddaoudi, M.; Kim, J. *Nature* **2003**, *423*, 705.

10.1021/ic048234x CCC: $30.25
Published on Web 06/02/2005

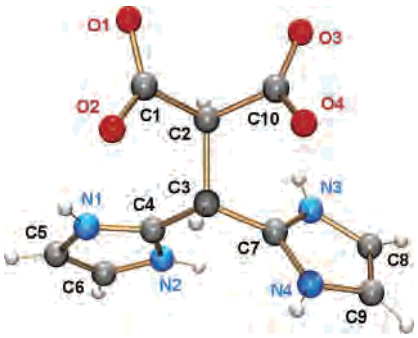

Figure 1. Structure of H_2DIMMAL with the atomic numbering scheme used in this work.

(MOFs) with interesting structural features, capable of leading to novel materials of potentially remarkable applications,[2] constitutes a challenging task of current interest for the inorganic chemist.

During the past few years, our research interest has focused mainly on the coordinating behavior of several ligands containing bis(imidazolyl) moieties. These kind of ligands form very stable complexes with 3d ions via the coordination of imidazole nitrogen atoms in six-membered chelate rings. In earlier works, we reported the results on the coordination chemistry of HBIP (HBIP = 3,3-bis(2-imidazolyl)propionic acid) and BIBM (bis(2-imidazolyl)bis(methoxycarbonyl)-methylmethane).[3]

As part of our continuing program of investigating the behavior of newly synthesized imidazole/carboxylate-based ligands, we describe herein the coordinating properties of DIMMAL (DIMMAL = 2-di1*H*-2-imidazolylmethylmalonate), as well as its ability to generate metal−organic coordination networks. DIMMAL can be described as a malonate backbone functionalized with two pendant imidazole groups. Figure 1 shows the structure of the H_2DIMMAL molecule with the atom numbering scheme used throughout this work. The malonate moiety (a 1,3-dicarboxylate anion) can act as a chelating bidentate ligand while simultaneously adopting a variety of carboxylato-bridging coordination modes. It has been shown to be a useful tool for connecting different metals and inducing a variety of magnetic interactions between them.[4−7] Depending on the pH and on the coordination ability of the metal center, either one or both carboxylic moieties can undergo deprotonation. The $-CO_2H$ and $-CO_2^-$ groups can behave as hydrogen bond donors as well as acceptors, generating the possibility of participating in intermolecular and intramolecular interactions to produce hydrogen-bonded metal coordination network structures. The simultaneous coexistence of carboxylate and carboxylic groups in the MBBs[2o] can be expected to facilitate their connectivity via the formation of $-CO_2^-\cdots$HOCO pairs. The two imidazole groups present in DIMMAL make it a flexible polydentate ligand of high denticity that can be expected to show a versatile coordination chemistry. In addition, the bulky groups, also present in DIMMAL, are handy for generating aromatic−aromatic interactions that would play an important role in the modulation of crystal packing. Thus, the combination of all of these multiple simultaneous modes of interactions (coordinative, H-bonding, and $\pi-\pi$, i.e., the three organizative forces usually involved in the formation of high-dimensional systems[1h,2k,l]) as the directional motifs guiding the self-assembly process make DIMMAL a particularly attractive structural support as a useful tool for the design of supramolecular networks.

Our previously reported initial results and the considerations mentioned above have led us to explore the potentialities of DIMMAL as a generator of multidimensional networks. We, herein, report the molecular and crystal structures and the properties of four new molecular compounds based on DIMMAL, H_2DIMMAL·H_2O (**1**), Na_2(DIMMAL)·$5H_2O$ (**2**), [Cu(HDIMMAL)$_2$] (**3**), and [Cu_2(DIMMAL)$_2$(H_2O)$_2$]·$2H_2O$ (**4**), whose 3D solid-state networks are held together by a combination of H-bonding and aromatic−aromatic interactions provided by the unique and convenient structural features of DIMMAL. In short, the 3D construction process of our DIMMAL derivatives can be schematically described as the result of the following three sequential steps (see Results and Discussion): (i) formation of MBBs by covalent interactions, (ii) linkage of MBBs into (1D) chains or (2D) sheets through multiple H-bonds essentially involving OH as the donor groups and oxygen atoms as the acceptors, and (iii) the 3D network structure resulting from stacking of the sheets along a given direction,

(2) (a) Braga, D.; Bazzi, C.; Maini, L.; Grepioni, F. *CrystEngComm* **1999**, 5. (b) Kahn, O.; Larionova, J.; Yakhmi, J. V. *Chem.—Eur. J.* **1999**, *5*, 3437. (c) MacDonald, J. C.; Malissa, P. C. D.; Pilley, M.; Foote, M. M.; Lundburg, J. L.; Henning, R. W.; Schultz, A. J.; Mansonpp, J. L. *J. Am. Chem. Soc.* **2000**, *122*, 47. (d) Robson, R. *J. Chem. Soc., Dalton Trans.* **2000**, 3735. (e) Desiraju, G. R. *J. Chem. Soc., Dalton Trans.* **2000**, 3745. (f) Holliday, B. J.; Mirkin, C. A. *Angew. Chem., Int. Ed.* **2001**, *40*, 2022. (g) Zaman, B.; Smith, M. D.; zur Loye, H.-C. *Chem. Mater.* **2001**, *13*, 3534. (h) Sunatsuki, Y.; Motoda, Y.; Matsumoto, N. *Coord. Chem. Rev.* **2002**, *226*, 199. (i) Janiak, C. *J. Chem. Soc., Dalton Trans.* **2003**, 2783. (j) Aakeroy, C. B.; Beatty, A. M.; Desper, J.; O'Shea, M.; Valdes-Martinez, J. *J. Chem. Soc., Dalton Trans.* **2003**, 3956. (k) Roesky, H. W.; Andruh, M. *Coord. Chem. Rev.* **2003**, *236*, 91. (l) Hosseini, M. W. *Coord. Chem. Rev.* **2003**, *240*, 157. (m) Öhrström, L.; Larsson, K. *J. Chem. Soc., Dalton Trans.* **2004**, 347. (n) Huang, Z.; Song, H.-B.; Du, M.; Chen, S.-T.; Bu, X.-H. *Inorg. Chem.* **2004**, *43*, 931. (o) Matthews, C. J.; Elsegood, M. R. J.; Bernardinelli, G.; Clegg, W.; Williams, A. F. *J. Chem. Soc., Dalton Trans.* **2004**, 492.

(3) (a) Gimeno, B.; Soto, L.; Sancho, A.; Dahan, F.; Legros, J.-P. *Acta Crystallogr.* **1992**, *C48*, 1671. (b) Gimeno, B.; Sancho, A.; Soto, L.; Legros, J.-P. *Acta Crystallogr.* **1996**, *C52*, 1226. (c) Sancho, A.; Gimeno, B.; Amigó, J. M.; Ochando, L. E.; Debaerdemaeker, T.; Folgado, J. V.; Soto, L. *Inorg. Chim. Acta* **1996**, *248*, 153. (d) Akhriff, Y.; Server-Carrió, J.; Sancho, A.; García-Lozano, J.; Escrivá, E.; Folgado, J. V.; Soto, L. *Inorg. Chem.* **1999**, *38*, 1174. (e) Akhriff, Y.; Server-Carrió, J.; Sancho, A.; García-Lozano, J.; Escrivá, E.; Soto, L. *Inorg. Chem.* **2001**, *40*, 6832. (f) Nuñez, H.; Timor, J.-J.; Server-Carrió, J.; Soto, L.; Escrivá, E. *Inorg. Chim. Acta* **2001**, *318*, 8.

(4) (a) Gil de Muro, I.; Mautner, F. A.; Insausti, M.; Lezama, L.; Arriortua, M. I.; Rojo, T. *Inorg. Chem.* **1998**, *37*, 3243. (b) Gil de Muro, I.; Insausti, M.; Lezama, L.; Urtiaga, K.; Arriortua, M. I.; Rojo, T. *J. Chem. Soc., Dalton Trans.* **2000**, 3360 and references therein. (c) Muro, I. G.; Insausti, M.; Lezama, L.; Pizarro, J. L.; Arriortua, M. I.; Rojo, T. *Eur. J. Inorg. Chem.* **1999**, 935.

(5) (a) Ruiz-Pérez, C.; Sanchiz, J.; Hernández-Molina, M.; Lloret, F.; Julve, M. *Inorg. Chem.* **2000**, *39*, 1363. (b) Ruiz-Pérez, C.; Hernández-Molina, M.; Lorenzo-Luis, P.; Lloret, F.; Cano, J.; Julve, M. *Inorg. Chem.* **2000**, *39*, 3845. (c) Sanchiz, J.; Rodriguez-Martin, Y.; Ruiz-Perez, C.; Mederos, A.; Lloret, F.; Julve, M. *New J. Chem.* **2002**, *26*, 1624 and references therein.

(6) Maji, T. K.; Sain, S.; Mostafa, G.; Lu, T.-H.; Ribas, J.; Monfort, M.; Chaudhuri, N. R. *Inorg. Chem.* **2003**, *42*, 709.

(7) Liu, T.-F.; Sun, H.-L.; Gao, S.; Zhang, S.-W.; Lau, T.-C. *Inorg. Chem.* **2003**, *42*, 4792.

Table 1. Bond Lengths (Å) and Angles (deg) for the H_2DIMMAL·H_2O Crystal

C(1)−O(1)	1.248(2)	C(4)−N(2)	1.334(2)
C(1)−O(2)	1.244(2)	N(1)−C(5)	1.372(2)
C(10)−O(3)	1.245(2)	C(5)−C(6)	1.340(2)
C(10)−O(4)	1.250(2)	C(6)−N(2)	1.371(2)
C(1)−C(2)	1.543(2)	C(7)−N(3)	1.328(2)
C(2)−C(10)	1.545(2)	C(7)−N(4)	1.326(2)
C(2)−C(3)	1.545(2)	N(3)−C(8)	1.374(2)
C(3)−C(4)	1.509(2)	C(8)−C(9)	1.341(2)
C(3)−C(7)	1.494(2)	C(9)−N(4)	1.373(2)
C(4)−N(1)	1.328(2)		
O(1)−C(1)−O(2)	125.8(1)	C(3)−C(4)−N(2)	127.7(1)
O(1)−C(1)−C(2)	116.9(1)	N(1)−C(4)−N(2)	107.7(1)
O(2)−C(1)−C(2)	117.4(1)	C(4)−N(1)−C(5)	109.4(1)
O(3)−C(10)−O(4)	124.9(1)	N(1)−C(5)−C(6)	106.6(1)
O(3)−C(10)−C(2)	117.7(1)	C(5)−C(6)−N(2)	107.8(1)
O(4)−C(10)−C(2)	117.4(1)	C(6)−N(2)−C(4)	108.5(1)
C(1)−C(2)−C(3)	112.2(1)	C(3)−C(7)−N(3)	127.6(1)
C(1)−C(2)−C(10)	107.5(1)	C(3)−C(7)−N(4)	124.4(1)
C(3)−C(2)−C(10)	110.8(1)	N(3)−C(7)−N(4)	107.9(1)
C(2)−C(3)−C(4)	111.4(1)	C(7)−N(3)−C(8)	109.0(1)
C(2)−C(3)−C(7)	111.8(1)	N(3)−C(8)−C(9)	106.9(1)
C(4)−C(3)−C(7)	110.9(1)	C(8)−C(9)−N(4)	107.2(1)
C(3)−C(4)−N(1)	124.5(1)	C(9)−N(4)−C(7)	109.0(1)

driven by H-bonds involving −NH (imidazole) as donors and $\pi-\pi$ interactions between the bulky groups in DIMMAL.

Results and Discussion

Crystal Structure of H_2DIMMAL·H_2O (1). The free ligand adopts its dizwitterion configuration and crystallizes as a monohydrate. Figure 1 shows the molecular diagram and labeling scheme of H_2(DIMMAL)·H_2O. Bond distances and angles are listed in Table 1. The zwitterion configuration is confirmed by the presence of hydrogen atoms bonded to all four imidazole nitrogen atoms, as shown by the difference Fourier map in which the hydrogen atoms where located. The fact that both carboxylate groups are essentially symmetric, with differences in the C−O distances of less than 3σ, also supports the dizwitterion configuration.

The imidazolium rings are planar with deviations from the mean planes of not greater than 0.003(1) Å. The ring C−C and C−N distances are comparable with those reported for several imidazolium salts[8] and related bis(imidazole) systems in the zwitterionic form.[3a,b,9] The dihedral angle between both aromatic rings is 110.3(1)°. As previously mentioned, the C−O bond distances in both carboxylate groups are very similar, suggesting that the negative charge is equally distributed on the fully ionized carboxylate group. The dihedral angle between the $-CO_2^-$ groups is 104.8(2)°.

The crystal packing of compound **1** is primarily determined by the H-bonds listed in Table 2. The linkage of H_2DIMMAL units by double N(3)···O(4) bridges generates chains running along the *z* direction (see Figure 2).

The crystallization water molecules (W5) are located between the chains linking them together into sheets parallel to the *bc* planes by hydrogen bonds. W5 acts as a H-donor for two O(3) atoms from different H_2DIMMAL molecules from two neighboring chains and as a H-acceptor for a third H_2DIMMAL molecule pertaining to one of the chains previously mentioned. Thus, each W5 molecule is H-bonded to three different MBBs generating the 2D framework displayed in Figure 2. Finally, these layers (L1, L2, and L3 in Figure 3) are connected, in the *a* direction, into the final 3D structure through the N(2)···O(1) interactions. The crystal packing is completed by $\pi-\pi$ interactions (see discussion below).

Table 2. Hydrogen Bonds for Compound **1**[a]

X−H···1Y	X−H (Å)	H···Y (Å)	X···Y (Å)	X−H···Y (deg)
O(5)−H(5A)···O(3)	0.86	2.01	2.865(2)	172
O(5)−H(5B)···O(3^{I})	0.96	1.88	2.824(2)	167
N(1)−H(1A)···O(5^{II})	0.88	2.07	2.801(2)	170
N(2)−H(2A)···O(1^{III})	0.86	1.85	2.680(2)	163
N(3)−H(3A)···O(4^{IV})	0.86	1.81	2.649(2)	164
N(4)−H(4A)···O(2^{V})	0.86	1.90	2.685(4)	152

[a] Symmetry operators: (I) $-x, -y, -z$; (II) $x, y+1, z$; (III) $x-1, y, z$; (IV) $-x, -y+1, -z+1$; and (V) $-x, -y+1, -z$.

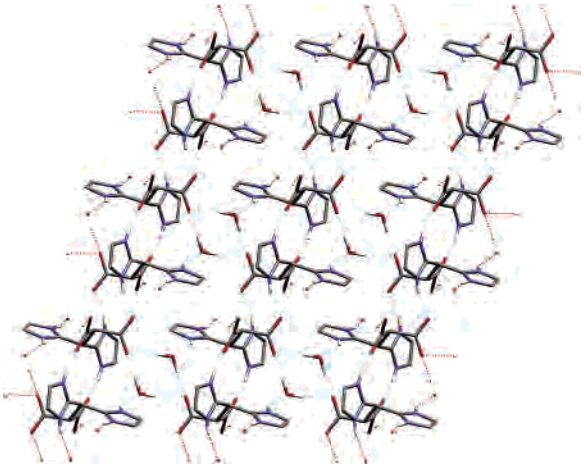

Figure 2. Two-dimensional network of compound **1** as viewed down the crystallographic *a* axis showing the extensive hydrogen bonding in the *bc* planes.

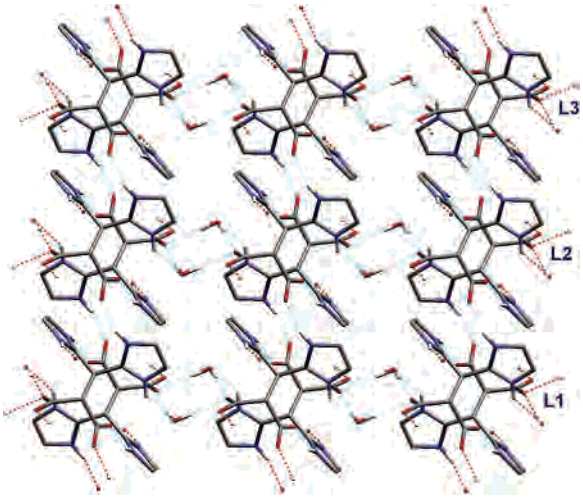

Figure 3. 3D framework of compound **1** as viewed along the *c* axis.

Crystal Structure of Na_2(DIMMAL)·$5H_2O$ (2). The disodium salt of DIMMAL can be described as being made

(8) Holbrey, J. D.; Reichert, W. M.; Tkatchenko, I.; Bouajila, E.; Walter, O.; Tommasi, I.; Rogers, R. D. *Chem. Commun.* **2003**, 28 and references therein.
(9) Koolhass, G. J. A.; Drieseen, W. L.; Reedijk, J. *Acta Crystallogr.* **1995**, *C51*, 918.

Table 3. Bond Lengths (Å) and Angles (deg) for the $Na_2(DIMMAL)\cdot 5H_2O$ Crystal[a]

Sodium Coordination			
Na(1)−O(1)	2.434(2)	Na(2)−O(1)	2.442(2)
Na(1)−O(5)	2.408(2)	Na(2)−O(3)	2.443(3)
Na(1)−O(6)	2.406(2)	Na(2)−O(5)	2.323(3)
Na(1)−O(7)	2.468(3)	Na(2)−O(9)	2.276(3)
Na(1)−O(8)	2.344(2)	Na(2)−O(6^{I})	2.596(3)
Na(1)−O(1^{I})	2.439(2)		
O(1)−Na(1)−O(5)	87.5(1)	O(7)−Na(1)−O(1^{I})	174.5(1)
O(1)−Na(1)−O(6)	84.6(1)	O(8)−Na(1)−O(1^{I})	90.8(1)
O(1)−Na(1)−O(7)	92.7(1)	O(1)−Na(2)−O(3)	79.3(1)
O(1)−Na(1)−O(8)	173.2(1)	O(1)−Na(2)−O(5)	89.2(1)
O(1)−Na(1)−O(1^{I})	83.1(1)	O(1)−Na(2)−O(9)	124.2(1)
O(5)−Na(1)−O(6)	168.2(1)	O(1)−Na(2)−O(6^{I})	80.4(1)
O(5)−Na(1)−O(7)	90.2(1)	O(3)−Na(2)−O(5)	116.8(1)
O(5)−Na(1)−O(8)	89.3(1)	O(3)−Na(2)−O(9)	95.1(1)
O(5)−Na(1)−O(1^{I})	86.0(1)	O(3)−Na(2)−O(6^{I})	153.6(1)
O(6)−Na(1)−O(7)	98.9(1)	O(5)−Na(2)−O(9)	138.5(1)
O(6)−Na(1)−O(8)	97.7(1)	O(5)−Na(2)−O(6^{I})	79.5(1)
O(6)−Na(1)−O(1^{I})	84.4(1)	O(9)−Na(2)−O(6^{I})	82.5(1)
O(7)−Na(1)−O(8)	93.2(1)		
DIMMAL Anion			
C(1)−O(1)	1.250(3)	C(4)−N(2)	1.317(3)
C(1)−O(2)	1.251(3)	N(1)−C(5)	1.371(3)
C(10)−O(3)	1.252(3)	C(5)−C(6)	1.343(3)
C(10)−O(4)	1.237(3)	C(6)−N(2)	1.395(3)
C(1)−C(2)	1.548(3)	C(7)−N(3)	1.321(3)
C(2)−C(10)	1.549(3)	C(7)−N(4)	1.335(3)
C(2)−C(3)	1.524(3)	N(3)−C(8)	1.384(3)
C(3)−C(4)	1.513(3)	C(8)−C(9)	1.341(3)
C(3)−C(7)	1.514(3)	C(9)−N(4)	1.369(3)
C(4)−N(1)	1.333(3)		
O(1)−C(1)−O(2)	125.5(2)	C(3)−C(4)−N(2)	129.1(2)
O(1)−C(1)−C(2)	114.1(2)	N(1)−C(4)−N(2)	111.3(2)
O(2)−C(1)−C(2)	120.4(2)	C(4)−N(1)−C(5)	108.4(2)
O(3)−C(10)−O(4)	124.7(2)	N(1)−C(5)−C(6)	105.3(2)
O(3)−C(10)−C(2)	115.5(2)	C(5)−C(6)−N(2)	110.3(2)
O(4)−C(10)−C(2)	119.6(2)	C(6)−N(2)−C(4)	104.6(2)
C(1)−C(2)−C(3)	114.3(2)	C(3)−C(7)−N(3)	128.6(2)
C(1)−C(2)−C(10)	103.0(2)	C(3)−C(7)−N(4)	120.6(2)
C(3)−C(2)−C(10)	110.8(2)	N(3)−C(7)−N(4)	110.8(2)
C(2)−C(3)−C(4)	112.8(2)	C(7)−N(3)−C(8)	105.2(2)
C(2)−C(3)−C(7)	109.9(2)	N(3)−C(8)−C(9)	110.1(2)
C(4)−C(3)−C(7)	109.9(2)	C(8)−C(9)−N(4)	105.6(2)
C(3)−C(4)−N(1)	119.6(2)	C(9)−N(4)−C(7)	108.3(2)

[a] Symmetry operator: (I) $-x, -y, -z$.

of centrosymmetric tetramers of sodium ions, $[Na_4(DIMMAL)_2(H_2O)_{10}]$. Bond distances and angles are listed in Table 3. A perspective view is shown in Figure 4. The central Na_4O_6 core motif has a prismatic structure composed of two Na-vacant face-sharing cubes in which Na and O atoms occupy alternate sites. The missing Na atoms are from two diagonally opposite corner sites of the prismatic structure, one on each cube.

The coordination around Na(1) adopts a distorted octahedral geometry with Na−O distances ranging from 2.344(2) to 2.468(3) Å (mean value of 2.42 Å). The O−Na−O angles range from 83.1 to 98.9° (average value of 89.9°). The distortion from the octahedral geometry is reflected by the angles between each pair of opposite O atoms and the central Na(1), which have values of 173.2(1), 174.5(1), and 168.2(1)° instead of the ideal 180°. The coordination polyhedron around Na(2) is strongly distorted, adopting a geometry that is intermediate between square pyramidal (SP) and trigonal bipyramidal (TBP). In the TBP configuration,

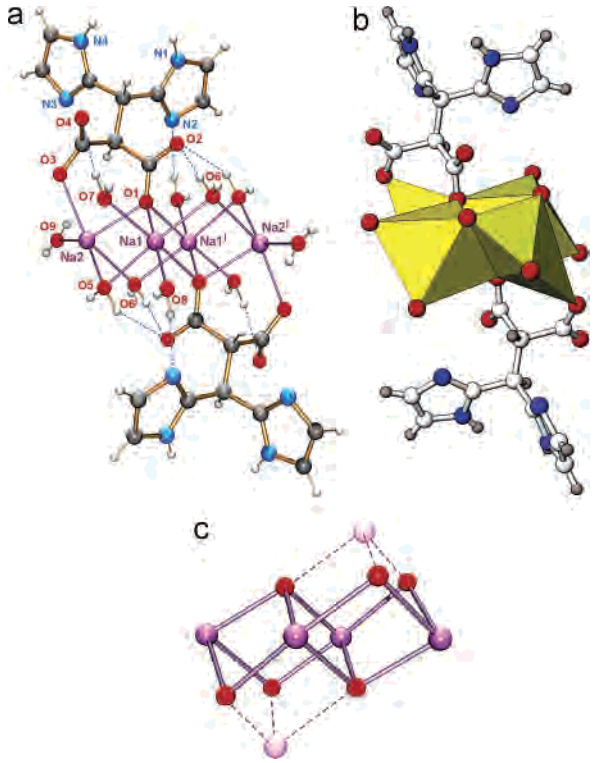

Figure 4. (a) ORTEP drawing of $[Na_4(DIMMAL)_2(H_2O)_{10}]$ showing the atom labeling scheme. Dashed blue lines show the intratetramer set of H-bonds (see text). (b) Representation of the tetramer moiety emphasizing the prismatic coordination polyhedra of the sodium atoms. (c) Representation of the Na_4O_6 core forming two face-sharing Na-vacant cubes.

O(3) and O(6^{I}) atoms occupy the axial positions, while O(1), O(5), and O(9) are equatorial. The Na−O distances range from 2.276(3) to 2.596(3) Å (mean value of 2.42 Å). The angles around the sodium atom in the equatorial plane vary from 89.2(1) to 138.5(1)° indicating a quite significant distortion from the ideal TPB geometry (120°). Moreover, the O(3)−Na(2)−O(6^{I}) angle (153.6°) is also very different from the ideal value of 180°. The distorted polyhedra around the sodium atoms are interconnected in an edge-sharing mode by carboxylate and water oxygen bridges. The shortest metal−metal distance within the tetramer is 3.401(2) Å. The geometry of the DIMMAL moieties (interatomic distances and angles) does not differ significantly from those previously reported for the H_2DIMMAL molecule as well as for the related HBIP and BIBM ligands.[3] As expected, the imidazole rings are planar with deviations from the mean planes not greater than 0.006(2) Å. The most significant differences between the protonated and deprotonated DIMMAL imidazole rings are the longer C(6)−N(2) and N(8)−N(3) bond distances found in the anionic form. The dihedral angle between the two imidazole rings of each ligand is 109.0(1)°. The C−O bond distances within the carboxylate groups range from 1.237(3) to 1.252(3) Å. One of the $-CO_2^-$ groups is almost symmetric (C(1)−O(1) and C(1)−O(2) bond distances of 1.250 and 1.251 Å, respectively), whereas the other one is slightly asymmetric (C(10)−O(3) and C(10)−O(4) bond distances of 1.252 and 1.237 Å, respectively).

Table 4. Hydrogen Bonds for Compound **2**[a]

X−H···Y	X−H (Å)	H···Y (Å)	X···Y (Å)	X−H···Y (deg)
O(5)−H(5A)···O(3^{II})	0.85	1.92	2.737(3)	161
O(5)−H(5B)···O(2^{I})	0.92	2.18	3.008(3)	150
O(6)−H(6A)···N(2^{III})	0.88	2.45	3.322(4)	170
O(6)−H(6B)···O(2)	0.84	1.96	2.777(3)	164
O(7)−H(7A)···N(3^{III})	0.89	2.09	2.963(4)	166
O(7)−H(7B)···O(4)	1.08	2.20	3.256(4)	168
O(8)−H(8A)···N(2^{I})	0.81	1.97	2.783(3)	175
O(8)−H(8B)···O(9^{III})	0.78	2.15	2.874(4)	154
O(9)−H(9A)···O(8^{IV})	0.73	2.34	2.874(4)	131
O(9)−H(9B)···O(3^{V})	0.74	2.47	3.004(4)	131
N(1)−H(1)···O(4^{VI})	0.86	2.05	2.867(3)	159
N(4)−H(4)···O(4^{VI})	0.86	2.11	2.915(3)	155

[a] Symmetry operators: (I) $-x, -y, -z$; (II) $-x-1, -y, -z$; (III) $x, y-1, z$; (IV) $x, y+1, z$; (V) $-x-1, -y+1, -z$; and (VI) $-x-1, -y, -z+1$.

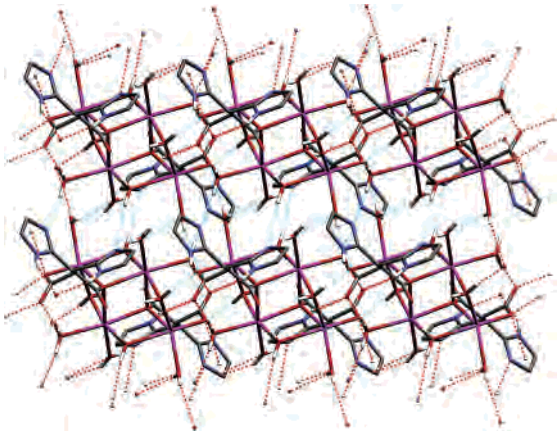

Figure 5. Packing diagram of $[Na_4(DIMMAL)_2(H_2O)_{10}]$ as viewed down the crystallographic *c* axis showing the extensive hydrogen bonding in the *ab* planes.

Compound **2** contains multiple H-bond donors/acceptors involving all of the water molecules as well as the imidazole nitrogen and the carboxylate oxygen atoms. Table 4 lists the H-bonds found in the crystal packing. Four of them are intratetramer (see Figure 4a), while the others connect the $[Na_4(DIMMAL)_2(H_2O)_{10}]$ blocks leading to the three-dimensional supramolecular network.

All 10 water molecules within the tetramer act as H-donors toward the different H-acceptors (water molecules, carboxylate anions, and nitrogen atoms) of the neighboring units. This set of hydrogen bonds originates the 2D structure of layers along the *ab* plane displayed in Figure 5.

Finally, the protonated nitrogen atoms of the imidazole groups participate in moderate hydrogen bonds as H-donors toward the carboxylate groups of neighboring building blocks. This set of H-bond contacts, in combination with the $\pi-\pi$ interaction between the imidazole rings (see below), link the *ab* layers (L1, L2, and L3, in Figure 6) described above into an infinite three-dimensional array.

Crystal Structure of [Cu(HDIMMAL)$_2$] (3). The structure of compound **3** consists of centrosymmetric mononuclear neutral $[Cu(HDIMMAL)_2]$ units linked together through hydrogen bonds involving the carboxylate and NH groups to give a three-dimensional network. Figure 7 shows a perspective view of the molecular unit with the atomic numbering scheme. Selected bond distances and angles are listed in Table 5.

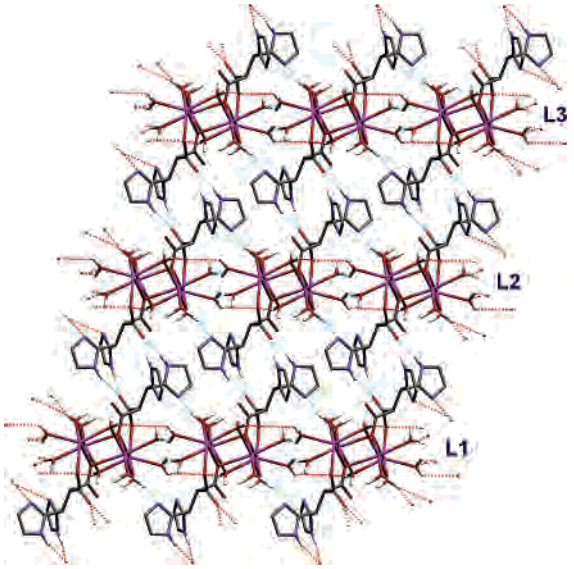

Figure 6. Topology of $[Na_4(DIMMAL)_2(H_2O)_{10}]$ with the 3D framework shown along the *b* axis.

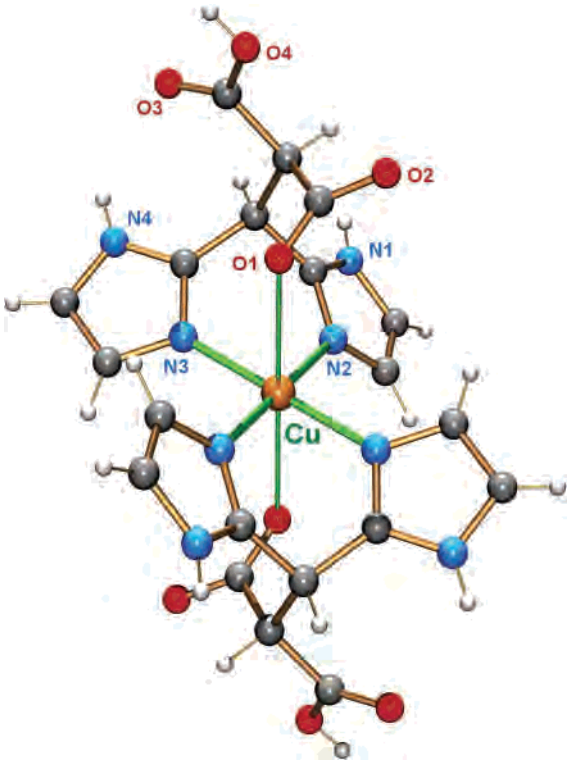

Figure 7. Perspective view and atomic numbering of the [Cu(HDIMMAL)$_2$] units.

The coordination around the copper atom adopts a tetragonally elongated octahedral geometry (4 + 2 coordination mode of CuN_4O_2 chromophores). The equatorial plane is made up of four nitrogen atoms from the imidazole ring with Cu−N bond distances of 1.989(2) and 1.997(2) Å. The axial sites are occupied by oxygen atoms from the carboxylate groups with a Cu−O distance of 2.530(2) Å. The tetragonality parameter, defined as the mean in-plane Cu−N bond length divided by the mean out-of-plane M−O bond length,[10]

Table 5. Selected Bond Lengths (Å) and Angles (deg) for Compounds **3** and **4**[a]

	[Cu(HDIMMAL)$_2$] (**3**)		
Cu−N(2)	1.997(2)	C(1)−O(1)	1.231(3)
Cu−N(3)	1.989(2)	C(1)−O(2)	1.285(3)
Cu−O(1)	2.530(2)	O(1)−C(1)−O(2)	124.3(2)
N(2)−Cu−N(3)	88.3(1)	C(10)−O(3)	1.203(3)
N(2)−Cu−O(1)	92.3(1)	C(10)−O(4)	1.323(3)
N(3)−Cu−O(1)	78.2(1)	O(3)−C(10)−O(4)	123.5(2)
	[Cu$_2$(DIMMAL)$_2$(H$_2$O)$_2$]·2H$_2$O (**4**)		
Cu−N(2)	1.980(4)	Cu−O(3^{I})	1.976(3)
Cu−N(3)	1.973(4)	Cu−O(5)	2.196(3)
Cu−O(1^{I})	1.984(3)		
N(2)−Cu−N(3)	88.5(2)	N(3)−Cu−O(3^{I})	169.1(1)
N(2)−Cu−O(1^{I})	166.5(1)	N(3)−Cu−O(5)	99.3(1)
N(2)−Cu−O(3^{I})	90.5(2)	O(1^{I})−Cu−O(3^{I})	88.4(1)
N(2)−Cu−O(5)	99.3(1)	O(1^{I})−Cu−O(5)	94.3(1)
N(3)−Cu−O(1^{I})	90.1(2)	O(3^{I})−Cu−O(5)	91.6(1)
C(1)−O(1)	1.281(4)	C(10)−O(3)	1.275(4)
C(1)−O(2)	1.230(4)	C(10)−O(4)	1.231(5)
O(1)−C(1)−O(2)	124.7(4)	O(3)−C(10)−O(4)	124.7(4)

[a] Symmetry operator: (I) $-x, -y, -z$.

is $T = 0.79$, in good agreement with those observed in the related CuN_4O_2 chromophores of imidazole-containing six-coordinate copper(II) complexes.[11−13]

The interatomic distances and angles within the DIMMAL moieties are similar to those found in the disodium salt previously described, except for the rotation of the C(2)−C(3) bond imposed by the interaction between Cu and O(1), as reflected by the H(2)−C(2)−C(3)−H(3) torsion angles being 58° in **3** compared with 9° in **2**. The imidazole rings are planar with deviations from the mean planes not greater than 0.003(2) Å. The dihedral angle between the two imidazole rings of each ligand is 125.7(1)°. The C−O$_{coord}$ distance is significantly shorter than the C−O$_{uncoord}$ distance (1.231(3) and 1.285(3) Å, respectively), which probably reflects the implication of the uncoordinated O(2) atoms in strong hydrogen bond interactions (see below) as well as the weakness of the Cu−O$_{coord}$ interaction. Otherwise, the C−O distances within the −CO$_2$H group are as expected for an un-ionized carboxylic group. The crystal packing of compound **3** (see Figures 8 and 9) is primarily determined by the H-bonds listed in Table 6.

The relatively simple hydrogen bond system can be attributed to the lack of water molecules of crystallization. The strongest H-bonds, O(4)−H(4A)···O(2^{I}) (d_{O-O} = 2.572 Å), corresponding to the predominately noncovalent[2o] carboxylic−carboxylate interactions interconnect the MBBs [Cu(HDIMMAL)$_2$]. Each molecular unit is involved in four such H-bonds, two as H-donors and two as H-acceptors, leading to the layered assemblage in the *bc* plane shown in Figure 8. The distance between neighboring Cu atoms within the layers is 10.49 Å. These layers, in turn, are further assembled into an infinite three-dimensional array via N-H···O hydrogen bonds and $\pi-\pi$ interactions (see below). Figure 9 shows the H-bond interactions between three adjacent layers (L1, L2, and L3) along the *b* axis. Finally, it should be noted that the O(2) atoms are involved in three H-bond interactions, two interlayer and one intralayer.

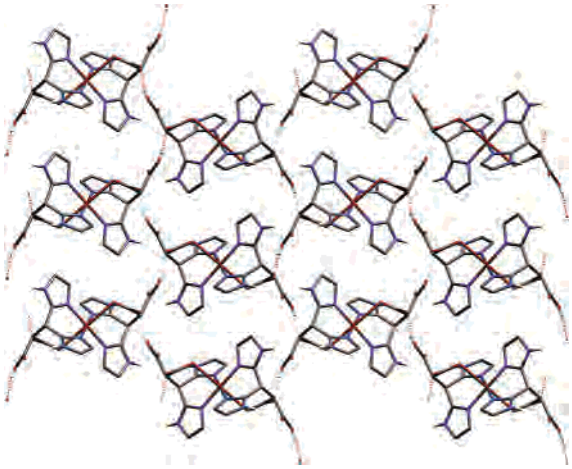

Figure 8. Packing diagram of compound **3** as viewed down the crystallographic *a* axis showing the extensive H-bonding in the *bc* planes.

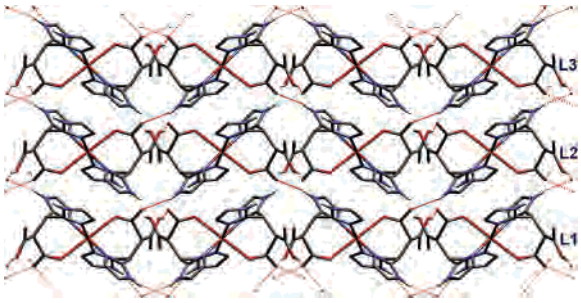

Figure 9. 3D framework of compound **3** shown along the *b* axis.

Table 6. Hydrogen Bonds for Compounds **3** and **4**[a]

X−H···Y	X−H (Å)	H···Y (Å)	X···Y (Å)	X−H···Y (deg)
	[Cu(HDIMMAL)$_2$] (**3**)			
O(4)−H(4A)···O(2^{I})	0.82	1.77	2.572(3)	165
N(1)−H(1)···O(2^{II})	0.86	2.05	2.855(3)	155
N(4)−H(4)···O(2^{III})	0.86	2.11	2.915(3)	155
	[Cu$_2$(DIMMAL)$_2$(H$_2$O)$_2$]·2H$_2$O (**4**)			
O(5)−H(5A)···O(6)	0.95	1.90	2.778(5)	153
O(5)−H(5B)···O(1^{IV})	0.83	1.90	2.721(4)	175
O(6)−H(6A)···O(3^{V})	1.02	1.95	2.824(5)	142
O(6)−H(6B)···O(5^{VI})	1.11	1.84	2.904(5)	158
N(1)−H(1)···O(4^{VII})	0.77	2.09	2.840(5)	165
N(4)−H(4)···O(2^{VII})	0.77	2.20	2.917(5)	155

[a] Symmetry operators: (I) $x, -y + 1/2, z - 1/2$; (II) $x + 1, -y + 1/2, z + 1/2$; (III) $x + 1, y, z$; (IV) $x, y + 1, z$; (V) $x - 1, y + 1, z$; (VI) $-x - 1, -y + 1, -z$; (VII) $-x, -y, -z - 1$.

Crystal Structure of [Cu$_2$(DIMMAL)$_2$(H$_2$O)$_2$]·2H$_2$O (4). The structure of compound **4** is composed of centrosymmetric dinuclear [Cu$_2$(DIMMAL)$_2$(H$_2$O)$_2$] motifs linked through hydrogen bonds involving water molecules as well as carboxylate and NH groups to give a three-dimensional network. Figure 10 shows a perspective view of the dinuclear cyclic unit and the atomic numbering scheme. Selected bond

(10) Hathaway, B. J In *Comprehensive Coordination Chemistry*; Wilkinson, G., Gillard, R. D., McCleverty, J. A., Eds.; Pergamon Press: Oxford, U.K., 1985; Vol. 5, p 601.
(11) Abuhijleh, A. L.; Woods, C. *Inorg. Chim. Acta* **1992**, *194*, 9.
(12) Place, C.; Zimmermann, J.-L.; Mulliez, E.; Guillot, G.; Bois, C.; Chottard, J.-C. *Inorg. Chem.* **1998**, *37*, 4030.
(13) Akhriff, Y. Ph.D. Thesis, University of Valencia, Valencia, Spain, 2004.

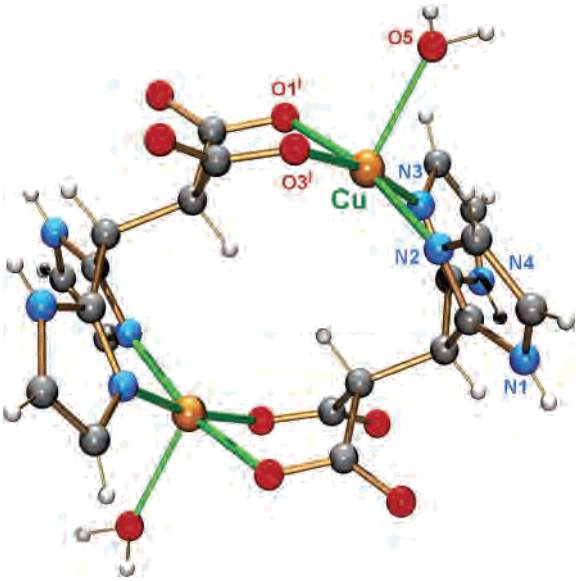

Figure 10. Perspective view and atomic numbering scheme of the $[Cu_2(DIMMAL)_2(H_2O)_2]$ dinuclear entities.

distances and angles are listed in Table 5. The two Cu atoms are linked together through the DIMMAL anions, which act as tetradentate-bridging ligands. The intradimeric copper−copper separation is 4.990(3) Å. This cyclic structure, formed by the bridging of the two metal centers by DIMMAL, may be considered to be a dinuclear metallamacrocycle.[14]

The coordination polyhedron around the copper(II) ions is a slightly distorted square pyramid. The basal plane is formed by two imidazole nitrogen atoms (N(2) and N(3)) and two oxygen atoms from different carboxylate groups (O(1) and O(3)). These four atoms are nearly coplanar with deviations from the least-squares plane of less than ±0.03 Å. The copper−oxygen and copper−nitrogen bond distances are normal (average 1.980 and 1.977 Å, respectively). The axial position is occupied by an oxygen atom from a water molecule with a Cu−O bond distance of 2.196(3) Å. As expected, the copper atom is displaced inward (0.21 Å) from the basal plane; the tetragonality parameter is $T = 0.90$. The distortion of the CuN_2O_2O' polyhedron can be quantified using the parameter τ as defined by Addison et al.[15] The calculated value of $\tau = 0.04$ ($\tau = 0$ for a regular SP and $\tau = 1$ for a regular TBP) indicates that SP is by far the prevalent geometry around the Cu atom.

The interatomic distances and angles of the DIMMAL moieties found in compound **4** are very similar to those found in compounds **2** and **3**, except, again, for the torsion angle H(2)−C(2)−C(3)−H(3) which is 0.6° for **4** compared to 9 and 58° for **2** and **3**, respectively. The imidazole rings are planar with deviations from the mean planes not greater than 0.003(2) Å. The dihedral angle between the two imidazole rings of each ligand is 129.2(1)°. Both carboxylate groups

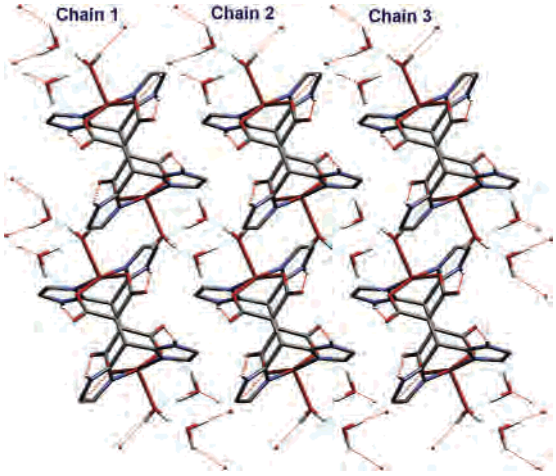

Figure 11. Two-dimensional network of compound **4** as viewed down the crystallographic *c* axis showing the extensive hydrogen bonding in the *ab* planes.

are unidentate with the C−O distances following the usual trend, $C-O_{coord} > C-O_{uncoord}$, as expected from the polarization of the charge density toward the metal-bonded oxygen atom.

Crystal packing is primarily induced by the hydrogen bonds listed in Table 6. Both types of water molecules, coordinated (W5) and crystallization (W6), are responsible for the formation of chains (1D) and sheets (2D) through their involvement in moderate hydrogen bonds, as indicated by the intermolecular O···O and O···H distances and the corresponding O−H···O angles. The W5 molecule acts as H-donor toward both W6 and the coordinated O(1) atom from the neighboring dinuclear moiety in the *y* axis. This double bridge W···O(1^{IV}) links each dinuclear motif to two others, above and below it, thus generating zigzag chains running along the [010] direction. The crystallization water molecules (W6) are located within the space between the chains, linking them together into sheets parallel to the *ab* plane by H-bond bridges between carboxylic oxygens and W5. Figure 11 shows the 2D framework originated by these interactions between the chains.

Also involved in H-bonding are the two N-H groups, N(1) and N(4),which act as H-donors toward uncoordinated O(4) and O(2) atoms from neighboring MBBs in the *c* axis (i.e., connecting the layers described above into the final 3D pattern shown in Figure 12). On top of that, aromatic−aromatic interactions between bulky groups constitute an additional factor playing a key role in the 3D self-assembly process, as discussed in the next paragraph.

Aromatic−Aromatic Interactions. Now, we consider the contribution of the aromatic−aromatic interactions to the stabilization of the crystal structure of the DIMMAL derivatives described above in more detail. The understanding of noncovalent interactions is of great importance in supramolecular chemistry.[1] In fact, the aromatic−aromatic interactions have been revealed to be as decisive as H-bonding in the modulation of three-dimensional networks.[1g] The four compounds described herein show several common structural features. In all of these cases, the network can be viewed as being built from 2D sheets by X−H···O linkages (X = N,

(14) Grosshans, P.; Jouaiti, A.; Bulach, V.; Planeix, J.-M.; Hosseini, M. W.; Kyritsakas, N. *Eur. J. Inorg. Chem.* **2004**, 453 and references therein.
(15) Addison, A. W.; Rao, T. N.; Reedijk, J.; Rijn, J., Verschoor, G. C. *J. Chem. Soc., Dalton Trans.* **1984**, 1349.

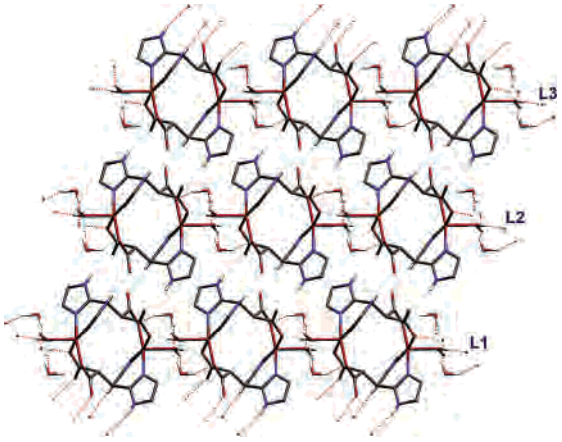

Figure 12. 3D framework of compound **4** viewed along the *a* axis.

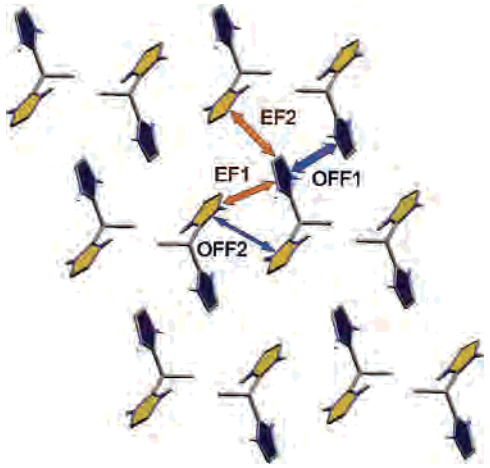

Figure 13. Schematic representation of the $\pi-\pi$ interactions in compound **1**.

O; also X−H···N in compound **2**) between their respective MBBs ([$(H_2$DIMMAL$)(H_2O)$], [Na_4(DIMMAL$)_2(H_2O)_{10}$], [Cu(HDIMMAL$)_2$], and [Cu_2(DIMMAL$)_2(H_2O)_2$] for compounds **1**, **2**, **3**, and **4**, respectively), further extended into a 3D supramolecular network by N−H···O and $\pi-\pi$ interactions.

The butterfly configuration of the bis(imidazolyl) fragments plays a determining role in the topological configuration of the 3D network. In compound **1** (Figure 13), each imidazolium ring interacts with three others from different bis(imidazolinium) groups, by three different modes, namely, two edge-to-face (EF1 and EF2) and one offset face-to-face (OFF1 between the rings containing N(1) and N(2) atoms and OFF2 between the rings with N(3) and N(4) atoms). Geometrical parameters characterizing these interactions are listed in Table 7. These interactions generate the *aromatic layers* shown in Figure 13, parallel to the (−101) plane. These layers could be considered as interpenetrating the H-bond-driven 2D sheets parallel to the (100) planes.

There are significant differences between the type of aromatic−aromatic interactions observed in the metal-organic derivatives (**2**, **3**, and **4**) and those in the free ligand. The aromatic groups, which are *outside* the sheets containing the metallic atoms and the coordinative interactions (see description of crystal structures), fill the gap between them making up intercalated aromatic layers between the sheets. The basic structural motif formed by these aromatic layers is very similar in all three metal-containing compounds, **2**−**4**: a rectangular *box* defined by two pairs of imidazole rings, each pair from a different bis(imidazolyl) group and related to each other by an inversion center (Figure 14). There are three interactions within each box, two (identical) edge-to-face (EF1) and one offset face-to-face (OFF1).

The rectangular $(\text{imidazole})_4$ *packs*, in turn, are associated to each other by means of a second edge-to-face interaction (EF2) generating 1D chains of boxes along one of the crystallographic axes (*a* in compounds **2** and **4**, *c* in compound **3**). Finally, a second offset face-to-face interaction (OFF2) in compounds **2** and **4** (but not in compound **3**) extends the 1D chains into a 2D framework. It should be pointed out that the γ's for OFF2 are greater than those for OFF1 (see Table 7).

Electron Spin Resonance Spectroscopy. The room-temperature Q-band spectrum of the polycrystalline samples of [Cu(HDIMMAL$)_2$] shows an axial-type signal ($g_{\|} = 2.228$, $g_{\perp} = 2.046$) with resolved hyperfine coupling in the parallel part of the spectrum ($A_{\|} = 194 \times 10^{-4}$ cm^{-1}). When the temperature is lowered to 120 K, the signal narrows but the *g* values remain practically unchanged. No half-field signal was detected. These results are consistent with a predominantly $d_{x^2-y^2}$ ground state for the Cu(II) ions in a statically distorted CuN_4O_2 polyhedron.[16] The observed EPR parameters are similar to those reported for related imidazole-containing copper(II) complexes.[11,13,17] A rough estimate of the σ-covalency factor, α (i.e., the mixing coefficient of the metal orbital $d_{x^2-y^2}$ in the ground-state molecular orbital), can be obtained by substitution of the esr experimental data ($A_{\|}$, taken as negative, $g_{\|}$ and $g_{\perp}$) into the well-known equation[18]

$$A_{\|} = P[(-K - 4/7)\alpha^2 + (g_{\|} - 2.0023) + (3/7)(g_{\perp} - 2.0023)]$$

where *K* is the Fermi contact term, with a value of 0.43, and *P* is a scaling factor estimated to be 0.036 cm^{-1} to yield the mixing coefficient $\alpha = 0.78$. This value indicates a moderate covalent Cu−ligand bond, within the range reported for most nitrogen/oxygen donor Cu(II) complexes.[19]

The room-temperature polycrystalline Q-band EPR spectrum of [Cu_2(DIMMAL$)_2(H_2O)_2]\cdot 2H_2O$ (**4**) shows a broad axial signal ($g_{\|} = 2.284$, $g_{\perp} = 2.057$, $g_{av} = 2.133$) with no hyperfine structure. Lowering the temperature to 120 K produces no effect on the shape and position of the signal.

(16) (a) Hathaway, B. J.; Billing, D. E. *Coord. Chem. Rev.* **1970**, *5*, 143. (b) Hathaway, B. J. *Struct. Bonding* **1984**, *57*, 55. (c) Hathaway, B. J. In *Comprehensive Coordination Chemistry;* Wilkinson, G., Ed.; Pergamon: Oxford, U.K., 1985; Vol. 5, p 604.
(17) McFadden, D. L.; McPhail, A. T.; Gross, P. M.; Garner, C. D.; Mabbs, F. E. *J. Chem. Soc., Dalton Trans.* **1976**, *1*, 47.
(18) Ozarowski, A.; Reinen, D. *Inorg. Chem.* **1985**, *24*, 3860.
(19) (a) Reinen, D.; Ozarowski, A.; Jakob, B.; Pebler, J.; Stratemeier, H.; Wieghardt, K.; Tolksdorf, I. *Inorg. Chem.* **1987**, *26*, 4010. (b) Steren, C. A.; Calvo, R.; Piro, O. E.; Rivero, B. E. *Inorg. Chem.* **1989**, *28*, 1933. (c) Atanasov, M.; Zotov, N.; Friebel, C.; Pretov, K.; Reinen, D. *J. Solid State Chem.* **1994**, *108*, 37.

Table 7. Geometrical Parameters of the Aromatic−Aromatic Interactions

		OFF1			OFF2			EF1	EF2
compound	α[a]	d_c[c] (Å)	d[d] (Å)	γ[b] (deg)	d_c[c] (Å)	d_p[d] (Å)	γ[b] (deg)	d_c[c] (Å)	d_c[c] (Å)
1	110.3	3.88	3.64	20.6	5.30	3.54	48.3	4.62	5.08
2	109.0	3.70	3.44	21.6	4.28	3.16	42.4	4.57	4.63
3	125.7	3.40	3.33	11.6	−	−	−	4.60	5.82
4	129.2	3.68	3.52	18.0	4.36	3.73	31.0	5.04	4.65

[a] α is the angle between two imidazole rings belonging to the same DIMMAL molecule. [b] γ is the angle between the centroid−centroid vector and the perpendicular to the imidazole nucleus plane. [c] d_c is the centroid-to-centroid distance. [d] d_p is the plane-to-plane distance.

The g values are in good agreement with those expected for a CuN_2O_2O' chromophore of roughly SP geometry and a $d_{x^2-y^2}$ ground state for the copper(II) ion.[16,20,21] When the spectrometer gain was increased, a weak-field signal of $\Delta M_s = 2$ at $g \approx 4.2$ is clearly observed, even at room temperature, which is consistent with weak low-dimensional magnetic interactions.

Magnetic Properties. The magnetic susceptibility of compound **3** exhibits a Curie−Weiss dependence. Fitting the susceptibility data to the expression $\chi = C/(T - \theta)$ gives the calculated values for $C = 0.422$ cm^3 mol^{-1} K and $\theta = -0.04$ K. The very small magnitude of the Weiss correction confirms the lack of any antiferromagnetic interactions between the copper(II) ions. From the Curie constant $C = N\beta^2g^2S(S + 1)/3k$ with $S = 1/2$, a g value of 2.12 can be obtained, which is in excellent agreement with the value obtained from the EPR spectrum.

A plot of $\chi_M T$ vs the temperature, for compound **4** (Figure 15), exhibits a slight decrease at $T < 8$ K, from 1.75 μ_B per Cu atom at 8 K to 1.32 μ_B per Cu atom at 1.8 K, which is consistent with weak antiferromagnetic interactions between the Cu(II) ions.

These results suggest that, from a magnetic point of view, the crystal structure of **4** should be described as an assembly of quasi-isolated dimers (see above). That is, the magnetic behavior of $[Cu_2(DIMMAL)_2(H_2O)_2]\cdot 2H_2O$ obeys a dimer exchange equation, such as eq 1. Because the exchange coupling constant is expected to be small (probably $|J| \approx g\mu_B H \approx 1$ cm^{-1}), the application of the Bleaney−Bowers[22] expression would be inappropriate. Instead, the magnetic data can be expected to fit the expression (1) derived from the exchange Hamiltonian $\hat{H} = 2J(\hat{S}_1\hat{S}_2) + g\mu_B H(\hat{S}_1 + \hat{S}_2)$ for a pair of exchange-coupled $S = 1/2$ ions that include the external field, H.[23]

$$\chi = [Ng\mu_B \sinh(g\mu_B H/kT)]\{H[\exp(-2J/kT) + 2\cosh(g\mu_B H/kT) + 1]\}^{-1} + N\alpha \quad (1)$$

In fact, when the magnetic data were least-squares fitted to this equation (solid line in Figure 15), after substitution of g by its experimental value from EPR, a $2J$ value of $-1.6(1)$ cm^{-1} was obtained with an agreement factor $R = 2.4 \times 10^{-4}$ (R is defined as $\sum[(\chi_M)_{obsd} - (\chi_M)_{calcd}]^2/\sum[(\chi_M)_{obsd}]^2$).

The low, but non-negligible, absolute value obtained for the $2J$ exchange parameter deserves a brief comment. At first, it might not be clear which dimensionality applies to the magnetic interactions because several exchange pathways, via covalent and noncovalent interactions, seem to be possible. Nevertheless, magnetic exchange interactions via noncovalent interdimeric interactions, such as hydrogen bonds and aromatic−aromatic interactions, can be ruled out. The main interdimeric interactions are through very extended bridging frameworks involving moderate hydrogen bonds with copper−copper distances (ranging from 6.9 to 9.2 Å) considerably longer than the intradimeric one (4.99 Å). The exchange-pathway distances are also too long. Only the triatomic bridges O(5)−H(5B)···O(1^{IV}) (see Table 6) could be considered suitable to propagate significant superexchange interactions.[24] Yet, the topology of the bridge framework suggests that the effectiveness of this interdimeric pathway should also be considered to be negligible. As discussed above, the unpaired electron of the copper(II) ion in **4** is essentially from a $d_{x^2-y^2}$ metallic orbital with very little contribution from the d_{z^2} orbital and is localized predominately in the basal plane. On the other hand, a superexchange via the electrons involved in the $\pi-\pi$ interactions seems to be rather unlikely for two main reasons. First, the topology of the pathway does not seem to be the most suitable because the angles between the imidazole rings and the equatorial CuN_2O_2 plane (where the spin density is essentially localized) are 37.5(2) and 39.4(2)°. Second, the presence of any magnetic interaction has been unequivocally ruled out in compound **3**, where similar Cu(imidazole)···(imidazole)Cu pathways are present (see above). Therefore, once the exchange pathways involving noncovalent interactions were rejected, the only possible apparent pathway for the observed weak antiferromagnetic coupling is a superexchange via the NC(im)−C−C−C−O bridges in the dinuclear entities. Coordination compounds showing significant through-bond coupling via C−C σ bonds between metallic ions are scarce. In fact, few Cu(II) complexes have been reported in which the metallic centers are linked via N−C−C−N sequences involving C−C σ bonds.[25,26] All of these systems display weak to moderate antiferromagnetic behavior, with the absolute values of the $2J$ parameters ranging from 7.8 to 47

(20) Escrivà, E.; Sanaú, M.; Folgado, J. V.; García-Lozano, J. *Polyhedron* **1996**, *15*, 3271.
(21) Mendoza-Díaz, G.; Driessen, W. L.; Reedijk, J.; Gorter, S.; Gasque, L.; Thompson, K. R. *Inorg. Chim. Acta* **2002**, *339*, 51.
(22) Bleaney, B.; Bowers, K. D. *Proc. R. Soc. London* **1952**, *A266*, 95.
(23) Myers, B. E.; Berger, L.; Friedberg, S. A. *J. Appl. Phys.* **1969**, *40*, 1149.
(24) Escrivà, E.; Server-Carrió, J.; García-Lozano, J.; Folgado, J.-V.; Sapiña, F.; Lezama, L. *Inorg. Chim. Acta* **1998**, *279*, 58 and references therein.
(25) (a) Chiari, B.; Hatfield, W. E.; Piovesana, O.; Tarantelli, T.; Haar, L. W.; Zanazzi, P. F. *Inorg. Chem.* **1983**, *22*, 1468. (b) Chiari, B.; Povesana, O.; Tarantelli, T.; Zanazzi, P. F. *Inorg. Chem.* **1984**, *23*, 2542.
(26) Colin, J. C.; Mallah, T.; Journaux, Y.; Lloret, F.; Julve, M.; Bois, C. *Inorg. Chem.* **1996**, *35*, 4176.

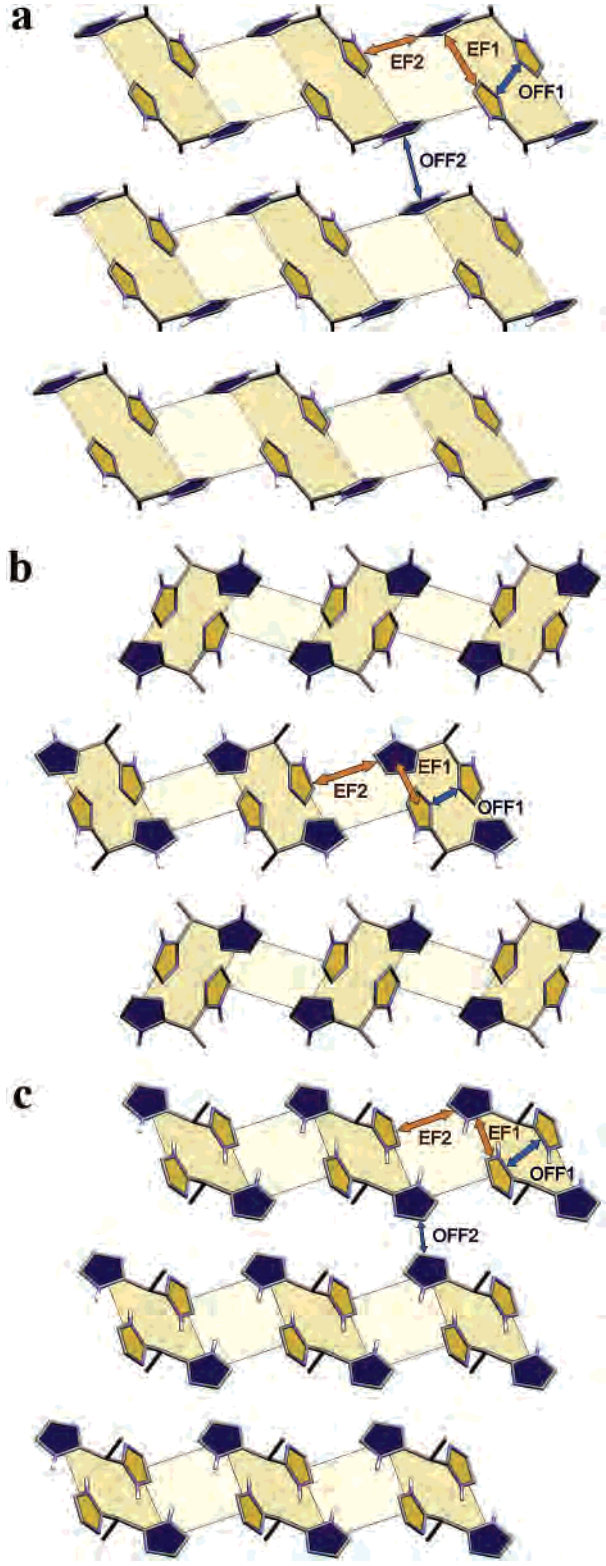

Figure 14. Schematic representation of $\pi-\pi$ interactions in (a) compound **2**, *ab* projection; (b) compound **3**, *cb* projection; and (c) compound **4**, *ac* projection.

cm^{-1}. The magnitude of the observed antiferromagnetic interaction in **4**, where the Cu(II) ions are linked by four quite long Cu···NC(im)−C−C−C−O···Cu sequences, although smaller, as expected, is certainly not negligible.

Conclusions. In summary, the present work successfully demonstrates the potential of DIMMAL as an efficient generator of multidimensional networks of novel MBBs, either by itself, as in **1**, or, more importantly, by interaction with metal ions, such as Na(I) in [Na_4(DIMMAL)$_2$(H_2O)$_{10}$] (**2**) and Cu(II) in [Cu(HDIMMAL)$_2$] (**3**) and [Cu_2(DIMMAL)$_2$-(H_2O)$_2$]·2H_2O (**4**). These MBBs possess the combination of structural features and capacities desired for extended multiple H-bonding and $\pi-\pi$ interactions between bulky groups. This work shows that both, multiple pathway H-bonding and $\pi-\pi$ interactions, constitute the key features in the stabilization of crystal packing. All of these characteristics cooperatively act to generate new 3D networks in the DIMMAL derivatives reported herein as the result of what can be described as a formal sequential process of three steps. First coordinative interactions form the MBBs which, in the second step, become interconnected into 1D chains or 2D layers by a multiple set of H-bonds involving essentially OH as the donor groups. Third, an additional set of H-bonds involving the (imidazole) NH groups together with the directional effects of the $\pi-\pi$ interactions between the bulky groups present in DIMMAL efficiently control the packing of the layers into a 3D network. These results taken together indicate that the presence of a metal ion, as well as its nature, constitutes an important factor in determining the solid structure and connectivities between the MBBs in each case. More systematic and extensive studies, currently in progress, using a variety of metal ions at different pHs, are needed to understand how they bear upon the building block structural motifs and their assembly process. This, in turn, should allow the control of the factors involved in the building process of high-dimensionality architectures.

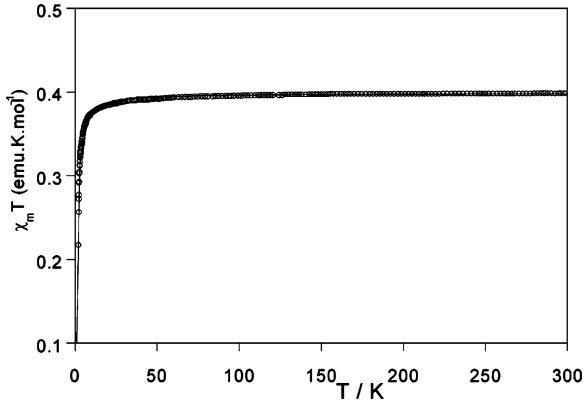

Figure 15. Temperature dependence of $\chi_M T$ for **4**.

Experimental Section

Physical Measurements. Polycrystalline powder EPR spectra (Q-band) were recorded on a Bruker ESP-300 spectrometer equipped with a variable-temperature device. Magnetic susceptibility was measured by means of a commercial SQUID magnetometer, Quantum Design model MPMS7, down to 1.8 K. Experimental susceptibilities were corrected for both the diamagnetic contribution, estimated from Pascal's constants,[27] and the TIP (taken as 60 × 10^{-6} cm^3 mol^{-1} per Cu(II)).

Preparation of H_2DIMMAL·H_2O (1). An aqueous solution of the sodic salt (see below) of ligand Na_2DIMMAL (0.5 mmol, 20

(27) Kahn, O. *Molecular Magnetism*; VCH Publishers: New York, 1993; p 3.

Table 8. Crystallographic Data for Compounds 1-4

	1	2	3	4
formula	$C_{10}H_{12}N_4O_5$	$C_{10}H_{18}N_4O_9Na_2$	$C_{20}H_{18}N_8O_8Cu$	$C_{20}H_{24}N_8O_{12}Cu_2$
fw	268.24	384.26	561.96	695.56
space group (No.)	$P\bar{1}$ (2)	$P\bar{1}$ (2)	$P2_1/c$ (14)	$P\bar{1}$ (2)
a (Å)	7.2689(2)	8.459(5)	7.2199(2)	8.0830(4)
b (Å)	8.9484(2)	8.664(5)	18.2281(5)	9.1351(4)
c (Å)	9.7317(4)	12.403(5)	10.4093(3)	9.1820(9)
α (deg)	114.66(1)	70.900(5)	90	71.99(1)
β (deg)	101.60(1)	72.290(5)	126.018(1)	75.60(1)
γ (deg)	92.86(1)	81.950(5)	90	83.33(1)
V (Å^3)	557.12(4)	817.4(8)	1108.03(5)	623.95(9)
Z	2	2	2	1
μ(Mo Kα) (mm^{-1})	0.130	0.178	1.054	1.787
ρ_{calcd} (g cm^{-3})	1.599	1.561	1.684	1.851
reflns collected	2210	5103	3225	2215
unique reflns [R(int)]	2185 [0.020]	4708 [0.023]	2638 [0.044]	2185 [0.015]
final R_1[a] value	0.0368	0.0687	0.0422	0.0465
final R_2[b] value	0.0936	0.1927	0.0923	0.0906

[a] $R_1 = \sum||F_o| - |F_c||/\sum|F_o|$ for reflections with $I > 2\sigma(I)$. [b] $R_2 = \{\sum[w(F_o^2 - F_c^2)^2]/\sum[w(F_c^2)^2]\}^{1/2}$ for all reflections; $w = 1/[\sigma^2(F_o^2) + (aP)^2 + bP]$, where $P = (2F_c^2 + F_o^2)/3$ and a and b are constants set by the program.

Scheme 1

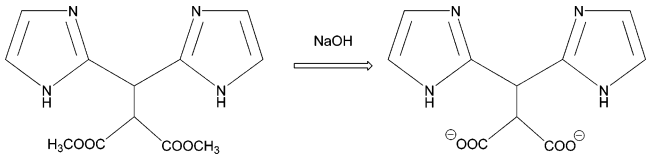

mL) was acidified with 1 M HCl to pH 2.72 and allowed to stand at room temperature for several hours to yield colorless crystals of the title compound, which were filtered, washed with cold ethanol, and dried.

Anal. Calcd for $C_{10}N_4O_5H_{12}$: C, 44.78; H, 4.51; N, 20.89. Found: C, 44.62; H, 4.42; N, 20.79.

Preparation of Na_2(DIMMAL)·5H_2O (2). Bis(2-imidazolyl)-bis(methoxycarbonyl)methylmethane (BIBM, Scheme 1) was prepared according to the method of Joseph et al.[28] and characterized by ^{1}H NMR, ^{13}C NMR, and IR spectroscopies. All other reagents were purchased from commercial sources. An aqueous solution of NaOH (20 mmol, 20 mL) was added dropwise to a methanolic suspension of BIBM (10 mmol, 10 mL) with stirring. Almost immediately, a yellow solution formed. Ethanol was then added until the solution yielded a white powder precipitate of compound **2**, which was filtered, washed with ethanol, and dried. The compound was characterized by ^{1}H NMR, ^{13}C NMR, and IR spectroscopies. The filtrate was left to stand at room temperature for several days to produce colorless crystals of compound **2**, which were separated by filtration.

Anal. Calcd for $C_{10}H_{18}N_4O_9Na_2$ (**2**): C, 31.26; H, 4.72; N, 14.58; Na, 11.97. Found: C, 31.17; H, 4.67; N, 14.52; Na, 11.89.

Preparation of [Cu(HDIMMAL)$_2$] (3) and [Cu_2(DIMMAL)$_2$-(H_2O)$_2$]·2H_2O (4). *Warning. Perchlorate salts are potentially explosive and should be handled only in small quantities and with care.* Aqueous solutions of Na_2(DIMMAL)·5H_2O (0.5 mmol, 15 mL) and $Cu(ClO_4)_2$ (0.25 mmol, 5 mL) were mixed resulting in a purple-blue solution. The pH was then adjusted to 6.0 with 0.1 M HCl. A blue polycrystalline powder appeared immediately, which was separated by filtration and washed with water and ethanol. Elemental analysis fits the formulation given for compound **4**. The solution immediately turns pale violet, and after 1 day thin violet crystals of **3** are obtained.

Crystals of **4** with a quality satisfactory for X-ray analysis were obtained according to the following procedure. Aqueous solutions of Na_2(DIMMAL)·5H_2O (0.5 mmol, 20 mL) and $Cu(ClO_4)_2$ (0.5 mmol, 5 mL) were mixed with stirring. A blue powder of **3** immediately precipitated and was filtered off. After standing at room temperature for 2 days, the resulting blue filtrate yielded X-ray quality blue crystals of **4**.

Anal. Calcd for $C_{20}H_{18}N_8O_8Cu$ (**3**): C, 42.74; H, 3.23; N, 19.94; Cu, 11.31. Found: C, 42.68; H, 3.17; N, 19.87; Cu, 11.19. Anal. Calcd for $C_{20}H_{24}N_8O_{12}Cu_2$ (**4**): C, 34.53; H, 3.48; N, 16.11; Cu, 18.28. Found: C, 34.47; H, 3.37; N, 16.02; Cu, 18.19.

Compound **3** can be also synthesized by the addition of an aqueous solution of Na_2(DIMMAL)·5H_2O to a water suspension of **4** until it is completely dissolved to yield a pale violet solution from which crystals of **3** are obtained.

X-ray Structure Determination. X-ray data sets for compounds **1**−**4** were collected on an Enraf-Nonius CAD4 single-crystal diffractometer, and intensity measurements were carried out at 293 K using graphite-monochromated Mo Kα radiation ($\lambda = 0.71070$ Å). The unit cell dimensions were determined from the angular settings of 25 reflections. The intensity data of the reflections were measured between the limits of $1° < \theta < 26°$ for **1**, $1° < \theta < 30°$ for **2**, $1° < \theta < 28°$ for **3**, and $1° < \theta < 25°$ for **4**, using the $\omega/2\theta$ scan technique. Data reduction was performed with the X-RAY76 System.[29] An empirical absorption correction was applied for compounds **3** and **4**, following the DIFABS procedure.[30] The structures were solved by direct methods using the SIR92[31] program and refined by the full-matrix least-squares method against F^2 with SHELXL97.[32] Non-hydrogen atoms were anisotropically refined. Hydrogens bonded to C atoms were placed at calculated positions, and hydrogens bonded to O and N atoms were located by difference synthesis. All of them were kept fixed in the refinement with isotropic temperature factors related to their bonded atom. Molecular graphical representations were produced with POV-Ray 3.5[33] working on files generated by ORTEP3 for Windows.[34] Packing

(28) Joseph, M.; Leigt, T.; Swain, M. L. *Synthesis* **1977**, 459.

(29) Stewart, J. M.; Machin, P. A.; Dickinson, C. W.; Ammon, H. L.; Heck, H.; Flack, H. *The X-RAY76 System*; Technical Report TR-446; Computer Science Center, University of Maryland: College Park, MD, 1976.

(30) Walker, N.; Stuart, D. *Acta Crystallogr.* **1983**, *A39*, 158.

(31) Altomare, A.; Burla, M. C.; Camalli, M.; Cascarano, G.; Giacovazzo, G.; Guagliardi, A.; Polidori, G. *J. Appl. Crystallogr.* **1994**, *27*, 435.

(32) Sheldrick, G. M. *SHELXL97*; University of Göttingen: Göttingen, Germany, 1997.

(33) Cason, C. J.; Froehlich, T.; Kopp, N.; Parker, R. *Persistence of Vision Raytracer for Windows*, version 3.5; POV−Team: Williamstown, Victoria, Australia, 2002.

(34) Farrugia, L. J. *J. Appl. Crystallgro.* **1997**, *30*, 565.

figures were produced with Mercury 1.2.[35] Other data relevant to the crystal structure study are listed in Table 8.

Acknowledgment. We thank Drs. C. Gómez and L. Lezama for their assistance with the magnetic susceptibility and EPR measurements, respectively. Financial support from the Dirección General de Investigación Científica y Técnica (Project BQU2003-01467) is gratefully acknowledged.

Supporting Information Available: Crystallographic data in CIF format. This material is available free of charge via the Internet at http://pubs.acs.org.

IC048234X

(35) Bruno, I. J.; Cole, J. C.; Edgington, P. R.; Kessler, M. K.; Macrae, C. F.; McCabe, P.; Pearson, J.; Taylor, R. *Acta Crystallogr*. **2002**, *B58*, 389.